cancer stem cells with metastatic capacity and a distinct molecular signature. Cancer Res. 2009; 69(4):1302-1313.

16. Croker AK, Goodale D, Chu J, Postenka C, Hedley BD, Hess DA and Allan AL. High aldehyde dehydrogenase and expression of cancer stem cell markers selects for breast cancer cells with enhanced malignant and metastatic ability. J Cell Mol Med. 2009; 13(8B):2236-2252.
17. Ponti D, Costa A, Zaffaroni N, Pratesi G, Petrangolini G, Coradini D, Pilotti S, Pierotti MA and Daidone MG. Isolation and in vitro propagation of tumorigenic breast cancer cells with stem/progenitor cell properties. Cancer Res. 2005; 65(13):5506-5511.
18. Mani SA, Guo W, Liao MJ, Eaton EN, Ayyanan A, Zhou AY, Brooks M, Reinhard F, Zhang CC, Shipitsin M, Campbell LL, Polyak K, Brisken C, Yang J and Weinberg RA. The epithelial-mesenchymal transition generates cells with properties of stem cells. Cell. 2008; 133(4):704-715.
19. Gupta PB, Onder TT, Jiang G, Tao K, Kuperwasser C, Weinberg RA and Lander ES. Identification of selective inhibitors of cancer stem cells by high-throughput screening. Cell. 2009; 138(4):645-659.
20. Calvet CY, Andre FM and Mir LM. The culture of cancer cell lines as tumorspheres does not systematically result in cancer stem cell enrichment. PLoS One. 2014; 9(2):e89644.
21. Soule HD, Maloney TM, Wolman SR, Peterson WD, Jr., Brenz R, McGrath CM, Russo J, Pauley RJ, Jones RF and Brooks SC. Isolation and characterization of a spontaneously immortalized human breast epithelial cell line, MCF-10. Cancer Res. 1990; 50(18):6075-6086.
22. Nishi M, Sakai Y, Akutsu H, Nagashima Y, Quinn G, Masui S, Kimura H, Perrem K, Umezawa A, Yamamoto N, Lee SW and Ryo A. Induction of cells with cancer stem cell properties from nontumorigenic human mammary epithelial cells by defined reprogramming factors. Oncogene. 2014; 33(5):643-652.
23. Cruz FD and Matushansky I. Solid tumor differentiation therapy - is it possible? Oncotarget. 2012; 3(5):559-567.
24. Takahashi K, Tanabe K, Ohnuki M, Narita M, Ichisaka T, Tomoda K and Yamanaka S. Induction of pluripotent stem cells from adult human fibroblasts by defined factors. Cell. 2007; 131(5):861-872.
25. Blagosklonny MV. Cancer stem cell and cancer stemloids: from biology to therapy. Cancer Biol Ther. 2007; 6(11):1684-1690.
26. Singh N, Bhalla M, de Jager P and Gilca M. An overview on ashwagandha: a Rasayana (rejuvenator) of Ayurveda. Afr J Tradit Complement Altern Med. 2011; 8(5 Suppl):208-213.
27. Sedelnikova OA, Horikawa I, Zimonjic DB, Popescu NC, Bonner WM and Barrett JC. Senescing human cells and ageing mice accumulate DNA lesions with unrepairable double-strand breaks. Nat Cell Biol. 2004; 6(2):168-170.
28. Leontieva OV, Lenzo F, Demidenko ZN and Blagosklonny MV. Hyper-mitogenic drive coexists with mitotic incompetence in senescent cells. Cell Cycle. 2012; 11(24):4642-4649.
29. Cowell JK, LaDuca J, Rossi MR, Burkhardt T, Nowak NJ and Matsui S. Molecular characterization of the t(3;9) associated with immortalization in the MCF10A cell line. Cancer Genet Cytogenet. 2005; 163(1):23-29.
30. Leontieva OV, Demidenko ZN and Blagosklonny MV. MEK drives cyclin D1 hyperelevation during geroconversion. Cell Death Differ. 2013; 20(9):1241-1249.
31. Leontieva OV, Demidenko ZN and Blagosklonny MV. S6K in geroconversion. Cell Cycle. 2013; 12(20):3249-3252.
32. Abbas T and Dutta A. p21 in cancer: intricate networks and multiple activities. Nat Rev Cancer. 2009; 9(6):400-414.
33. Kondo T. Stem cell-like cancer cells in cancer cell lines. Cancer Biomark. 2007; 3(4-5):245-250.
34. Medema JP. Cancer stem cells: the challenges ahead. Nat Cell Biol. 2013; 15(4):338-344.
35. Kaul MK, Kumar A, Ahuja A, Mir BA, Suri KA and Qazi GN. Production dynamics of Withaferin A in Withania somnifera (L.) Dunal complex. Nat Prod Res. 2009; 23(14):1304-1311.
36. Vyas AR and Singh SV. Molecular targets and mechanisms of cancer prevention and treatment by withaferin a, a naturally occurring steroidal lactone. AAPS J. 2014; 16(1):1-10.
37. Hahm ER, Lee J, Kim SH, Sehrawat A, Arlotti JA, Shiva SS, Bhargava R and Singh SV. Metabolic alterations in mammary cancer prevention by withaferin A in a clinically relevant mouse model. J Natl Cancer Inst. 2013; 105(15):1111-1122.
38. Oh JH, Lee TJ, Kim SH, Choi YH, Lee SH, Lee JM, Kim YH, Park JW and Kwon TK. Induction of apoptosis by withaferin A in human leukemia U937 cells through down-regulation of Akt phosphorylation. Apoptosis. 2008; 13(12):1494-1504.
39. Lee J, Sehrawat A and Singh SV. Withaferin A causes activation of Notch2 and Notch4 in human breast cancer cells. Breast Cancer Res Treat. 2012; 136(1):45-56.
40. Roy RV, Suman S, Das TP, Luevano JE and Damodaran C. Withaferin A, a steroidal lactone from Withania somnifera, induces mitotic catastrophe and growth arrest in prostate cancer cells. J Nat Prod. 2013; 76(10):1909-1915.
41. Kim SH and Singh SV. Mammary Cancer Chemoprevention by Withaferin A Is Accompanied by In Vivo Suppression of Self-Renewal of Cancer Stem Cells. Cancer Prev Res (Phila). 2014.
42. Arden KC. FoxO: linking new signaling pathways. Mol Cell. 2004; 14(4):416-418.
43. Cheng T, Rodrigues N, Shen H, Yang Y, Dombkowski D, Sykes M and Scadden DT. Hematopoietic stem cell quiescence maintained by p21cip1/waf1. Science. 2000; 287(5459):1804-1808.
44. Liu M, Casimiro MC, Wang C, Shirley LA, Jiao X, Katiyar S, Ju X, Li Z, Yu Z, Zhou J, Johnson M, Fortina P, Hyslop T, Windle JJ and Pestell RG. p21CIP1 attenuates Ras- and

c-Myc-dependent breast tumor epithelial mesenchymal transition and cancer stem cell-like gene expression in vivo. Proc Natl Acad Sci U S A. 2009; 106(45):19035-19039.

45. Roninson IB. Tumor cell senescence in cancer treatment. Cancer Res. 2003; 63(11):2705-2715.

46. Serrano M. Cancer: a lower bar for senescence. Nature. 2010; 464(7287):363-364.

47. Rodier F and Campisi J. Four faces of cellular senescence. J Cell Biol. 2011; 192(4):547-556.

48. Vazquez-Martin A, Lopez-Bonetc E, Cufi S, Oliveras-Ferraros C, Del Barco S, Martin-Castillo B and Menendez JA. Repositioning chloroquine and metformin to eliminate cancer stem cell traits in pre-malignant lesions. Drug Resist Updat. 2011; 14(4-5):212-223.

49. Del Barco S, Vazquez-Martin A, Cufi S, Oliveras-Ferraros C, Bosch-Barrera J, Joven J, Martin-Castillo B and Menendez JA. Metformin: multi-faceted protection against cancer. Oncotarget. 2011; 2(12):896-917.

50. Yang J, Mani SA, Donaher JL, Ramaswamy S, Itzykson RA, Come C, Savagner P, Gitelman I, Richardson A and Weinberg RA. Twist, a master regulator of morphogenesis, plays an essential role in tumor metastasis. Cell. 2004; 117(7):927-939.

51. Smit MA and Peeper DS. Epithelial-mesenchymal transition and senescence: two cancer-related processes are crossing paths. Aging (Albany NY). 2010; 2(10):735-741.

52. Ansieau S, Bastid J, Doreau A, Morel AP, Bouchet BP, Thomas C, Fauvet F, Puisieux I, Doglioni C, Piccinin S, Maestro R, Voeltzel T, Selmi A, Valsesia-Wittmann S, Caron de Fromentel C and Puisieux A. Induction of EMT by twist proteins as a collateral effect of tumor-promoting inactivation of premature senescence. Cancer Cell. 2008; 14(1):79-89.

53. Lee KE and Bar-Sagi D. Oncogenic KRas suppresses inflammation-associated senescence of pancreatic ductal cells. Cancer Cell. 2010; 18(5):448-458.

54. Polyak K and Weinberg RA. Transitions between epithelial and mesenchymal states: acquisition of malignant and stem cell traits. Nat Rev Cancer. 2009; 9(4):265-273.

55. Trost TM, Lausch EU, Fees SA, Schmitt S, Enklaar T, Reutzel D, Brixel LR, Schmidtke P, Maringer M, Schiffer IB, Heimerdinger CK, Hengstler JG, Fritz G, Bockamp EO, Prawitt D, Zabel BU, et al. Premature senescence is a primary fail-safe mechanism of ERBB2-driven tumorigenesis in breast carcinoma cells. Cancer Res. 2005; 65(3):840-849.

56. Ryo A, Uemura H, Ishiguro H, Saitoh T, Yamaguchi A, Perrem K, Kubota Y, Lu KP and Aoki I. Stable suppression of tumorigenicity by Pin1-targeted RNA interference in prostate cancer. Clin Cancer Res. 2005; 11(20):7523-7531.

57. Nishi M, Akutsu H, Masui S, Kondo A, Nagashima Y, Kimura H, Perrem K, Shigeri Y, Toyoda M, Okayama A, Hirano H, Umezawa A, Yamamoto N, Lee SW and Ryo A. A distinct role for Pin1 in the induction and maintenance of pluripotency. J Biol Chem. 2011; 286(13):11593-11603.

STEM CELLS TRANSLATIONAL MEDICINE

EMBRYONIC STEM CELLS/INDUCED PLURIPOTENT STEM (iPS) CELLS

Removal of Reprogramming Transgenes Improves the Tissue Reconstitution Potential of Keratinocytes Generated From Human Induced Pluripotent Stem Cells

KEN IGAWA,[a,b] CHIKARA KOKUBU,[c] KOSUKE YUSA,[d] KYOJI HORIE,[c] YASUHIDE YOSHIMURA,[c] KAORI YAMAUCHI,[e] HIROFUMI SUEMORI,[e] HIROO YOKOZEKI,[b] MASASHI TOYODA,[f] NOBUTAKA KIYOKAWA,[f] HAJIME OKITA,[f] YOSHITAKA MIYAGAWA,[f] HIDENORI AKUTSU,[f] AKIHIRO UMEZAWA,[f] ICHIRO KATAYAMA,[a] JUNJI TAKEDA[c]

[a]Department of Dermatology and [c]Department of Social and Environmental Medicine, Graduate School of Medicine, Osaka University, Osaka, Japan; [b]Department of Dermatology, Graduate School of Medicine, Tokyo Medical and Dental University, Tokyo, Japan; [d]Wellcome Trust Sanger Institute, Wellcome Trust Genome Campus, Hinxton, Cambridge, United Kingdom; [e]Department of Embryonic Stem Cell Research, Institute for Frontier Medical Sciences, Kyoto University, Kyoto, Japan; [f]Department of Reproductive Biology, Center for Regenerative Medicine, National Center for Child Health and Development, Tokyo, Japan

Correspondence: Ken Igawa, M.D., Ph.D., Department of Dermatology, Graduate School of Medicine, Tokyo Medical and Dental University, 1-5-45 Yushima, Bunkyo-ku, Tokyo 113-8519, Japan. Telephone: 81-3-5803-5286; E-Mail: k.igawa.derm@tmd.ac.jp; or Junji Takeda, M.D., Ph.D., Department of Social and Environmental Medicine, Graduate School of Medicine, Osaka University, 2-2 Yamadaoka, Suita-city, Osaka 565-0871, Japan. Telephone: 81-6-6879-3262; E-Mail: takeda@mr-envi.med.osaka-u.ac.jp

Received October 2, 2013; accepted for publication May 21, 2014; first published online in SCTM EXPRESS July 14, 2014.

1066-5099/2014/$20.00/0

http://dx.doi.org/10.5966/sctm.2013-0179

Key Words. Human • Induced pluripotent stem cell • Keratinocyte • Differentiation • Transgene

ABSTRACT

Human induced pluripotent stem cell (hiPSC) lines have a great potential for therapeutics because customized cells and organs can be induced from such cells. Assessment of the residual reprogramming factors after the generation of hiPSC lines is required, but an ideal system has been lacking. Here, we generated hiPSC lines from normal human dermal fibroblasts with *piggyBac* transposon bearing reprogramming transgenes followed by removal of the transposon by the transposase. Under this condition, we compared the phenotypes of transgene-residual and -free hiPSCs of the same genetic background. The transgene-residual hiPSCs, in which the transcription levels of the reprogramming transgenes were eventually suppressed, were quite similar to the transgene-free hiPSCs in a pluripotent state. However, after differentiation into keratinocytes, clear differences were observed. Morphological, functional, and molecular analyses including single-cell gene expression profiling revealed that keratinocytes from transgene-free hiPSC lines were more similar to normal human keratinocytes than those from transgene-residual hiPSC lines, which may be partly explained by reactivation of residual transgenes upon induction of keratinocyte differentiation. These results suggest that transgene-free hiPSC lines should be chosen for therapeutic purposes. STEM CELLS TRANSLATIONAL MEDICINE *2014;3:992–1001*

INTRODUCTION

Reprogramming of differentiated somatic cells into a pluripotent state has been previously carried out by cell fusion or nuclear transfer [1]. The molecular basis of reprogramming has been revealed by exogenous expression of combinations of transcription factors. Recently, four factors, namely *OCT4*, *SOX2*, *KLF4*, and c*MYC*, which are highly expressed in embryonic stem cells (ESCs), have been shown to reprogram both mouse and human somatic cells into ESC-like pluripotent cells, named induced pluripotent stem cells (iPSCs) [2, 3].

ESCs have an unlimited proliferative capacity and extensive differentiation capability and are thought to be a powerful cell source for regenerative medicine [4]. However, there are both ethical and biological concerns for the clinical use of ESCs that are related to their derivation from embryos and potential for immunological rejection, respectively. In addition, it is difficult to generate patient- or disease-specific ESCs that are required for their effective application. These disadvantages can be at least partially avoided by the alternative use of iPSCs.

Induction of reprogramming by defined factors has been mostly carried out by coinfection with retroviral vectors [2, 3]. The major problems of this retrovirus-based method are its oncogenicity and mutagenesis. Reactivation of the proviral *Myc* oncogene is one of the reasons for the oncogenicity of iPSCs [5]. However, although three-factor (*Oct4*, *Sox2*, and *Klf4*) iPSC-derived mice do not develop tumors [6], ectopic expression of any one of these genes may have deleterious consequences. For example, ectopic expression of Oct4 in the skin or intestine causes tumor development [7]. Overexpression of Klf4 induces dysplasia of the skin [8]. Furthermore, retroviral integration itself causes insertional mutagenesis and may alter the expression pattern of nearby genes [9]. Therefore, transgene integration-free iPSCs are necessary for their clinical use.

To achieve such iPSCs, we used the *piggyBac* transposon system to deliver the reprogramming

factors. The *piggyBac* transposon is a moth-derived DNA transposon [10] that is highly active in mammalian cells and that has been used for gene delivery and mutagenesis [11]. The advantage over viral integration is that transposons can be easily removed from the host genome. Among the various DNA transposons, the *piggyBac* transposon does not leave "footprint" mutations upon excision [12]. The TTAA integration sites used by *piggyBac* transposons are repaired to the original sequence upon excision [12], resulting in removal of transposons from the host genome without changing any nucleotide sequences. Using this *piggyBac* transposon system, transgene integration-free and mutation-free mouse iPSCs have already been generated and reported by some groups, including our own [13–15].

In this study, by exploiting this unique property of the *piggyBac* transposon system, we generated transgene-free (Tg−) human induced pluripotent stem cell (hiPSCs) from transgene-retaining (Tg+) parental hiPSCs, thereby preserving the common isogenic genetic background. We generated epidermal keratinocytes from both Tg− and Tg+ hiPSCs in vitro and directly compared their tissue reconstitution potentials, allowing precise evaluation of the net effect of residual transgenes in hiPSCs and their derivatives.

Materials and Methods

Plasmid Construction

Five human reprogramming factors (*POU5F1*, *SOX2*, *KLF4*, *cMYC*, and *LIN28*) were amplified by polymerase chain reaction (PCR) with fusion of the first and second half of the T2A sequence in the C and N termini, respectively, except for the N terminus of *POU5F1* and the C terminus of *LIN28*. PCR products were cloned into pCR4 using a Zero Blunt Topo PCR cloning kit (Life Technologies, Rockville, MD, http://www.lifetech.com), resulting in pCR-O, pCR-S, pCR-K, pCR-M, and pCR-L, respectively. The sequences of the inserts were verified by capillary sequencing. To combine all five factors into a single coding sequence, the BglII-SalI fragment containing the SOX2-coding sequence in pCR-S was first cloned into the BamHI-SalI site of pCR-O, resulting in pCR-OS. KLF4, MYC, and LIN28 fragments were sequentially inserted in the same manner, resulting in the final construct, pCR-OSKML (h5F). The EcoRI-SalI fragment of h5F was cloned into the EcoRI-SalI site of pBluescript, resulting in pBS-h5F. The BamHI-SalI fragment of pBS-h5F was cloned into the BglII-XhoI site of the *piggyBac* transposon vector, pPB-CAG.EBNXN, resulting in PB-CAG-h5F. Finally, the negative selection marker PGK-puΔtk cassette was excised from pFlexible [16] by XhoI digestion and then inserted into the SalI site of pPB-CAG-h5F, resulting in pPB-CAG-h5F-puroTK. Primers for construction of the vectors are listed in supplemental online Table 1.

Cell Culture

Mouse embryonic fibroblasts (MEFs) were cultured in Dulbecco's modified Eagle's medium (DMEM) containing 10% fetal bovine serum (Life Technologies), 2 mM L-glutamine, 1× nonessential amino acids (Life Technologies), and 0.1 mM 2-mercaptoethanol. Normal human dermal fibroblasts (NHDFs) (Lonza, Walkersville, MD, http://www.lonza.com) from neonatal male skin were cultured in the same medium. Normal human epidermal keratinocytes (Lonza), also from neonatal male skin, and keratinocytes derived from iPSCs (iKCs) were cultured in serum-free keratinocyte-specific medium (CnT57; CELLnTEC, Bern, Switzerland, http://cellntec.com). Human iPSC lines and ESC lines (KhES-1 and KhES-3; Kyoto University, Kyoto, Japan, http://www.kyoto-u.ac.jp/en [17]) were cultured on mitomycin C-treated MEFs in serum-free human ESC (hESC) medium consisting of DMEM/F-12 (Life Technologies) with 20% knockout serum replacement (Life Technologies), 2 mM L-glutamine, 1× nonessential amino acids (Life Technologies), 0.1 mM 2-mercaptoethanol, and 5 ng/ml basic fibroblast growth factor (bFGF) (Katayama Chemical Industries Co., Ltd., Osaka, Japan, http://www.katayamakagaku.co.jp).

Generation of hiPSCs

Generation of hiPSCs was conducted according to the protocol described in Figure 1. NHDFs were plated in six-well plates and grown to 60%–70% confluence. On day 0, 2.5 μg of pCMV-mPBase and plasmids containing the *piggyBac* transposon carrying the reprogramming factors (pPB-CAG-h5F-puroTK) were simultaneously transfected into cells using Lipofectamine 2000 (Life Technologies) according to the manufacturer's protocol. On day 5, transfected NHDFs were trypsinized and replated onto feeder cells (1×10^5 MEFs per 60-mm dish) in serum-free hESC medium. The medium was refreshed every other day. On days 10–14, ESC-like colonies appeared in the dishes, and at approximately day 21, colonies were counted, picked, and expanded further.

Preparation of Splinkerettes

Splinkerettes were prepared by annealing Spl-top and Spl-blunt (to generate blunt ends). The sequences of these oligonucleotides are listed in supplemental online Table 1. After heat denaturation at 95°C for 10 minutes, annealing was performed by cooling down the mixture of 11 pmol of each strand in 10 mM Tris-HCl (pH 7.4) and 5 mM $MgCl_2$ in a total volume of 100 μl.

Determination of Transposon Integration Sites

Transposon integration sites were determined by splinkerette PCR. Genomic DNA from primary iPSCs was digested by appropriate restriction enzymes (HaeIII and RsaI) for 2 hour in 20-μl reactions. After heat inactivation, 2 μl of the digestion mixture was ligated with the 0.5 μl of splinkerette adaptors in 20-μl reactions. One microliter of the ligation mixture was then subjected to nested PCR. A primer pair, Spl-P1 and PB5-P1, was used for the first PCR. In the second PCR, the Spl-P2 and PB5-P2 primer pair was used (primer sequences are listed in supplemental online Table 1). Finally, PCR products were directly sequenced to determine the genomic sequences flanking the *piggyBac* terminal repeats. Sequences were analyzed by Blat searching the UCSC Genome Browser.

Bisulfite Sequencing Analysis

Bisulfite conversion of DNA was performed using a MethylEasy Xceed Rapid DNA Bisulphite Modification Kit (Genetic Signatures, Randwick, Australia, http://geneticsignatures.com) according to the manufacturer's protocol, and then sequencing was performed. Primers for amplification of bisulfited DNA are listed in supplemental online Table 1.

Southern Blot Analysis

To detect the copy number of integrated transposons, genomic DNA from each hiPSC line was digested and hybridized with

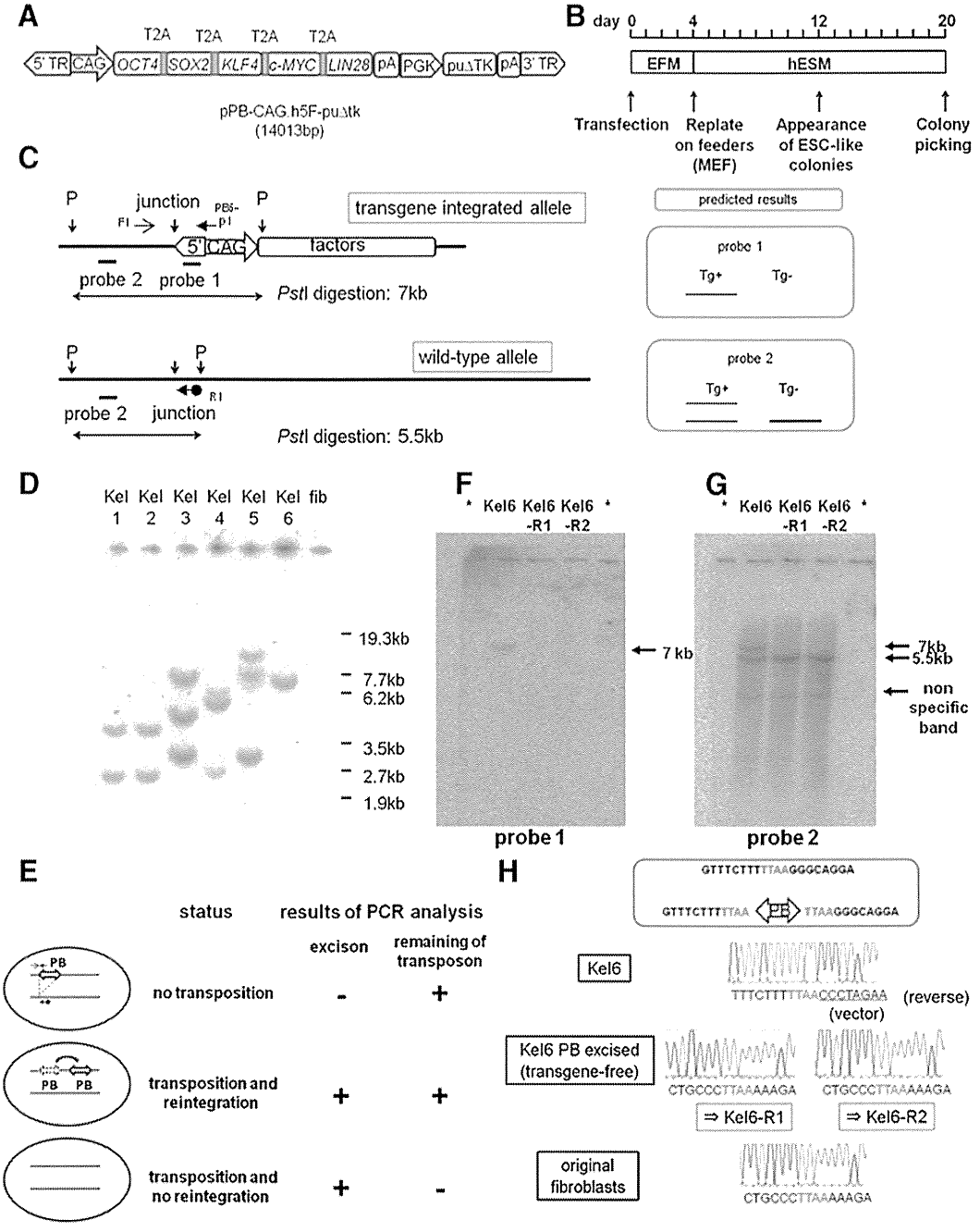

Figure 1. Generation of human induced pluripotent stem cells (hiPSCs) using the *piggyBac* transposon system and establishment of transgene-free hiPSCs. **(A):** Schematic representation of the *piggyBac* transposon vector carrying reprogramming factors (pPB-CAG.h5F-puΔtk, 14,013 bp). Genes encoding five factors were linked by sequences encoding 2A peptides. Expression of these factors was driven by constitutively active CAG promoters. **(B):** Timeline of reprogramming. **(C):** Representative restriction enzyme map and positions of primers used to evaluate transposon removal in the hiPSC genome at the site of transposon vector integration. Probes 1 and 2 were designed as indicated by the thick line. A schematic representation of the predicted results of Southern blot analysis using probe 1/2 is shown (right). The thick line indicates a higher density band. F1, R1, and PB5-p1 are primers used to evaluate transposon removal. Primer sequences are listed in supplemental online Table 1. **(D):** Southern blot analysis of primary hiPSCs. Genomic DNA was digested with PstI and hybridized with probe 1. Lanes 1–6, primary hiPSCs generated by transposon-mediated reprogramming. Lane 7, original fibroblast genomic DNA as a negative control. **(E):** Schematic representation of the strategy of transposon removal. Each arrow indicates a designated primer used for a two-step PCR screening (Fig. 1C; supplemental online Fig. 2). Representative PCR results for each status are shown in supplemental online Fig. 3. **(F, G):** The results of Southern blot analysis indicating transposon-free hiPSCs were confirmed by PCR screening. **(F)** and **(G)** show the results using probes 1 and 2, respectively. Lanes marked by asterisks contained sample loading buffer only (without DNA). **(H):** Sequencing analysis of the integration site on chromosome 7 in Kel6 and transposon-excised Kel6 (Kel6-R1 and Kel6-R2). The reference sequences (top) indicate the transposon integration sites where TTAA sequences were duplicated at both ends of the transposon. The electrophoretograms demonstrate that the sequences in Kel6-R1 and Kel6-R2 are identical to the original sequences in the fibroblasts and reference sequences. Abbreviations: EFM, embryonic fibroblast medium; ESC, embryonic stem cell; fib, fibroblast; hESM, human embryonic stem cell medium; junction, junction site of the genome and transposon vector; MEF, mouse embryonic fibroblast; p, PstI; PB, *piggyBac* transposon vector; PCR, polymerase chain reaction; puΔtk, puΔtk expression cassette; Tg+, transgene-residual; Tg−, transgene-free; 3′TR, 3′ terminal repeat of the *piggyBac* transposon; 5′TR, 5′ terminal repeat of the *piggyBac* transposon.

partial sequences of the *piggyBac* transposon 5′ terminal repeat as the probe. Primer sequences for generating the probe are listed in supplemental online Table 1.

Transposon Removal From Primary hiPSCs

Fifteen micrograms of the *piggyBac* transposase expression vector with the blasticidin (bsd) selection cassette was electroporated into 1×10^6 dissociated hiPSCs. A total of 2×10^5 cells were seeded onto 6-cm dishes containing feeder cells (MEFs) in hESC medium containing 10 μM ROCK inhibitor. From the following day, 2 μg/ml bsd was added to the culture medium, and selection was continued for 3 days. After an additional 7 days of culture without bsd, the resulting colonies were dissociated to single cells and expanded in hESC medium containing 10 μM ROCK inhibitor. Transposon removal was screened by two-step PCR analysis with the primers listed in supplemental online Table 1. The results of the PCR screening were confirmed by Southern blot analysis using the 5′ terminal repeat of the *piggyBac* transposon as one of the probes and genomic sequences just outside of the transposon integration site as the other probe. Primer sequences for generating the probe are listed in supplemental online Table 1.

Keratinocyte Induction From hiPSCs

We used the differentiation protocol described in Results to obtain keratinocytes from hiPSCs and hESCs. One week of random differentiation was induced in differentiation medium (hESC medium without bFGF). Then the culture medium was changed to serum-free keratinocyte-specific medium, and the cells were cultured for an additional 4–5 weeks.

Immunostaining

Cells were fixed in 3% formaldehyde in phosphate-buffered saline (PBS) for 15 minutes at room temperature and then permeabilized in 100% methanol for 10 minutes at −20°C when needed. Then the cells were blocked in serum-free protein block (Dako, Glostrup, Denmark, http://www.dako.com) for 1 hour at room temperature. The cells were incubated with antibodies against NANOG (Cell Signaling Technology, Beverly, MA, http://www.cellsignal.com; 1:200, rabbit polyclonal), OCT4 (Cell Signaling Technology; 1:200, rabbit polyclonal), SOX2 (Cell Signaling Technology, 1:200, rabbit polyclonal), SSEA4 (Cell Signaling Technology; 1:200, mouse IgG3 monoclonal), TRA-1-60 (Cell Signaling Technology; 1:200, mouse IgM monoclonal), TRA-1-81 (Cell Signaling Technology; 1:200, mouse IgM monoclonal), human keratin 5/14 (Covance, Princeton, NJ, http://www.covance.com; 1:500, rabbit IgG polyclonal), and each negative control antibody (Dako) overnight at 4°C. After washing with PBS (three times for 5 minutes), cells were labeled with Alexa Fluor 488- or Alexa Fluor 555-conjugated secondary antibodies (Life Technologies) for 1 hour at room temperature. After washing with PBS (three times for 5 minutes), specimens were analyzed under a fluorescence microscope (BZ-9000 BIOREVO; Keyence, Osaka, Japan, http://www.keyence.com).

Deparaffinized and rehydrated tissue sections were immersed in preheated (~100°C) target retrieval solution (Dako) for 10 minutes. After cooling at room temperature, the sections were washed three times with PBS, and nonspecific binding sites were blocked by incubation with serum-free protein block for 1 hour at room temperature. Then the sections were incubated with antibodies against human keratin 14 or involucrin (GeneTex, San Antonio, TX, http://www.genetex.com; 1:500, rabbit IgG polyclonal) at 4°C overnight. After three washes with PBS, tissue sections were reacted with an Alexa Fluor 555-conjugated secondary antibody for 1 hour at room temperature. After further washing, the sections were mounted with Fluoprep (bioMérieux, Marcy l'Etoile, France, http://www.biomerieux.com).

Real-Time PCR

Total RNA was extracted using an SV Total RNA Isolation System (Promega, Madison, WI, http://www.promega.com). One microgram of total RNA was reverse transcribed using random primers by Moloney murine leukemia virus reverse transcriptase (Life Technologies) and then subjected to PCR using the primers listed in supplemental online Table 1. Quantitative RT-PCR was performed using Power SYBR Green PCR Master Mix (Life Technologies) and an ABI7900HT sequence detector (Life Technologies) according to the manufacturer's protocols. Quantification of gene expression was based on the ΔCt method and normalized to β-actin expression. Melting curve and electrophoresis analyses were undertaken to verify the specificities of the PCR products and to exclude nonspecific amplification.

Single-Cell Gene Expression Analysis (Fluidigm Dynamic Array)

Single-cell gene expression profiling was performed using a Biomark dynamic array (Fluidigm, South San Francisco, CA, http://www.fluidigm.com) according to the manufacturer's protocol. Briefly, the cells were single-cell sorted using a BD FACSAria (BD Biosciences, San Diego, CA, http://www.bdbiosciences.com) into 2× CellsDirect buffer (Life Technologies). Cells were subjected to target-specific reverse transcription and 18 cycles of PCR preamplification with a mix of primers specific to the target genes (STA). STA products were then processed for real-time PCR analysis on Biomark 48:48 dynamic array integrated fluidic circuits (Fluidigm). The results obtained from the analysis were conducted with the R statistics package and output as a heat map. The primers for the analysis are listed in supplemental online Table 2.

RESULTS

Successful Establishment of hiPSCs Using the *piggyBac* Transposon System

To deliver the reprogramming factors to recipient cells, we constructed *piggyBac* transposon-based reprogramming vectors as described in Materials and Methods (Fig. 1A). cDNAs constituting the open reading frames of *OCT4*, *SOX2*, *KLF4*, *cMYC*, and *LIN28* were combined into a single open reading frame separated by sequences encoding 2A peptides and placed under the constitutively active CAG promoter. The ~20-amino acid 2A peptides from the *Thosea asigna* virus (T2A) work as self-cleaving signals and enable the expression of several gene products from a single transcript [18], thereby facilitating multigene delivery to target cells.

NHDFs were transfected with the above-mentioned *piggyBac* transposon vector carrying the five factors to induce reprogramming. The protocol we used is illustrated in Figure 1B. We performed cationic lipofection to introduce 2.5 μg of *piggyBac*

transposon and 2.5 μg of *piggyBac* transposase expression vector into ~70% confluent NHDFs cultured in six-well plates and maintained the cells in embryonic fibroblast medium for 4 days. At day 5, the transfected NHDFs were replated onto feeder cells (mitomycin C-treated MEFs) and maintained in human ESC (hESC) medium. At approximately day 14, small ESC-like colonies appeared. At day 20, colonies were picked up and passaged. In summary, we transfected 1×10^5 NHDFs with a transfection efficiency of approximately 10%, which was confirmed with the preliminary results using green fluorescent protein as reporter, and obtained approximately 100 colonies. Therefore, the overall reprogramming efficiency was approximately 1%, which is virtually equivalent to that of the retroviral method.

Derivation of Transgene Integration-Free and Mutation-Free hiPSCs by *piggyBac* Transposon Vector Removal

We investigated the copy number of the integrated transposons by Southern blot analysis with a probe designed in the 5′ repeat of the *piggyBac* transposon (probe 1 in Fig. 1C). As shown in Figure 1D, most hiPSCs colonies had multiple insertions. Among the colonies, we obtained a colony with single-copy integration (named KeI6). In the following experiments, our established hiPSC clone, KeI6, or its derivatives were mainly used.

To obtain transgene-free hiPSCs, we first used splinkerette PCR to identify the integration sites and found that the transposon was integrated at chromosome 7 (supplemental online Fig. 1). Next, we attempted to eliminate transposons from the hiPSC genome. As described in Materials and Methods, we used a two-step PCR screening system to select transposon-free iPSCs after transfection of the *piggyBac* transposase expression plasmid (Fig. 1E). The first PCR was conducted with a primer pair that detected excision of the transposon from the original site (Fig. 1C). The second PCR was conducted with a primer pair that detected the transposon itself (supplemental online Fig. 2). Representative results of this PCR screening are shown in supplemental online Figure 3.

After transient transposase expression and bsd selection, because transposase expression vector possesses bsd selection cassette, we picked colonies and screened them by PCR as described above. We obtained 10 clones of 55 colonies from the transposase-transfected KeI6 line, in which excision of the transposon had occurred (positive in the first step PCR analysis). After the second PCR analysis, we obtained two transposon-free candidate clones of the 10 clones. We then expanded two transposon-free clones (named KeI6-R1 and KeI6-R2) and confirmed them by Southern blot analysis using the 5′ repeat of the *piggyBac* transposon as the probe (probe 1 in Fig. 1C). We confirmed the loss of transposons in both clones that we identified as transposon-free by PCR (Fig. 1F). We also performed further Southern blot analysis using a probe designed just outside of the transposon-genome junction (probe 2 in Fig. 1C), which confirmed the results described above (Fig. 1G). Thus, we concluded that the transposons had been successfully removed in KeI6-R1 and KeI6-R2.

The *piggyBac* transposon does not leave a footprint at the excised site. To confirm that the transgene-free hiPSCs had no footprint mutations, we amplified the genomic regions encompassing the integration excision sites by PCR and then sequenced the PCR products directly. If there was a footprint mutation (e.g., a nucleotide change, insertion, or deletion), the sequence after TTAA, the target site of *piggyBac* integration, would be a mixture of sequences from the wild-type and excised alleles. The signals from all integration sites were identical to those from the original genomic sequence (Fig. 1H), indicating the absence of footprint mutations. Thus, we "cured" transgene-harboring hiPSCs by removing the transposon.

Characteristics of the Established hiPSCs

Next, we investigated the characteristics of the established hiPSCs. Immunofluorescence staining showed that both transgene-residual and -free hiPSC lines uniformly expressed stem cell markers such as OCT4, SOX2, NANOG, and SSEA4 (Fig. 2A). We also conducted RT-PCR analysis of *OCT4* and *NANOG* gene expression and found that these genes were expressed in our hiPSCs at approximately the same levels as those in retrovirus-based hiPSCs, whereas gene expression associated with the transposon appeared to be silenced (Fig. 2B; supplemental online Fig. 2). To evaluate the epigenetic reprogramming status, we investigated the DNA methylation status at *OCT4* promoter regions by bisulfite sequencing analysis and found that these promoter regions were almost completely unmethylated in the hiPSCs, which was in contrast to the status of the original fibroblasts (58% of the CpGs were methylated; Fig. 2C). This result indicated that the epigenetic reprogrammed status was maintained in our established hiPSCs even after the transgenes were eliminated. As shown in Figure 2D, karyotypic analysis revealed that both KeI6 and KeI6-R1 had a normal karyotype, 46XY. To confirm the pluripotency of the hiPSCs, we performed in vitro differentiation analysis. Both transgene-residual and -free hiPSC lines successfully differentiated into the three germ layers, namely ectoderm (K14-positive cells), mesoderm (desmin-positive cells), and endoderm (α-fetoprotein-positive cells) (Fig. 2E). These results suggested that the transgene-residual and -free hiPSC lines had phenotypes similar to those of pluripotent cells in terms of gene expression, epigenetic modifications, and the potential for differentiation into the three germ layers.

Keratinocyte Induction From hiPSCs

We next attempted to differentiate the established hiPSCs into epidermal keratinocytes. There are few reports that describe protocols for differentiation of hiPSCs or hESCs into keratinocytes, in which retinoic acid (RA) and/or bone morphogenetic protein 4 (BMP4) are preferably used [19, 20]. In the present study, as described in Materials and Methods, we used a modified protocol in which neither RA nor BMP4 were used; this protocol is briefly illustrated in Figure 3A. At 4–5 weeks after induction of the differentiation, we obtained cells that had a keratinocyte-like morphology. These cells proliferated and were passaged at least five times in serum-free keratinocyte medium without feeder cells. Moreover, these cells were positive for K5/K14 as indicated by immunohistochemistry (Fig. 3D), suggesting successful differentiation of keratinocytes from hiPSCs. We called these cells induced keratinocytes (iKCs).

Comparing our established transgene-residual iKCs with transgene-free iKCs, there were obvious morphological differences in which transgene-residual iKCs showed a somewhat spindle-shaped morphology (Fig. 3B). Subsequent culturing resulted in transgene-residual iKCs showing a more spindle-shaped morphology. Moreover, some morphologically undifferentiated colonies were developing in the culture (Fig. 3C). Therefore, we checked

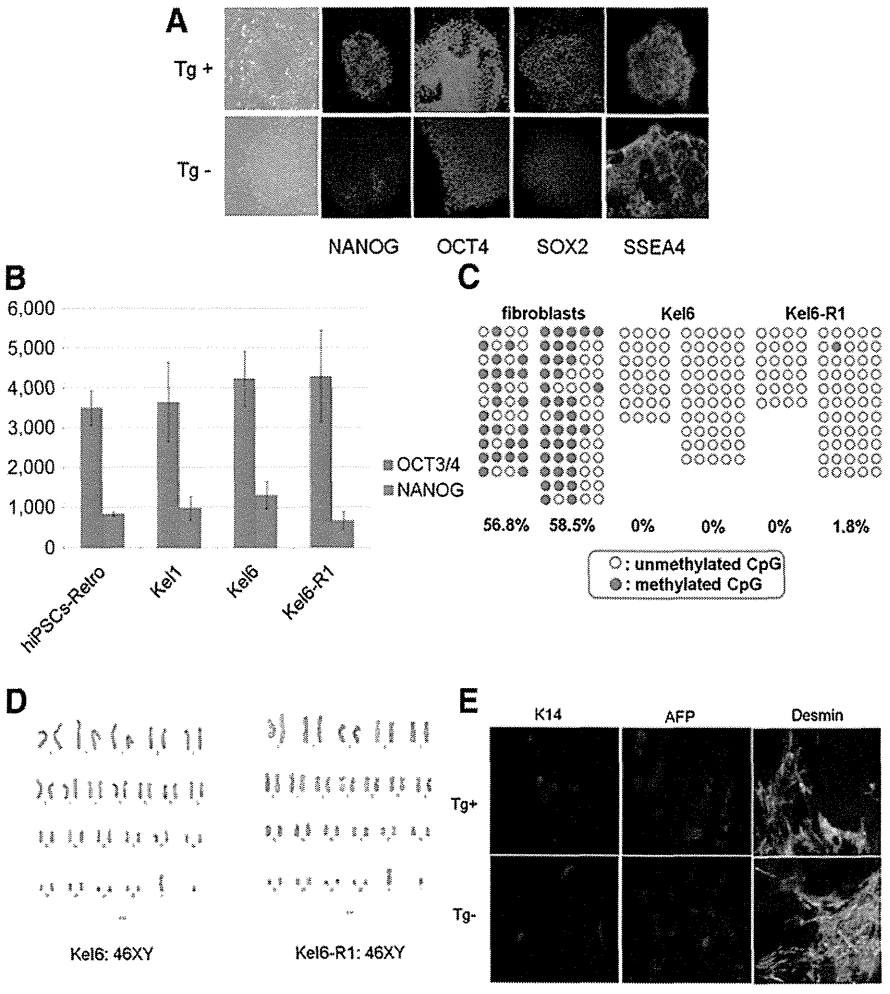

Figure 2. Characteristics of the established hiPSCs. **(A):** Immunofluorescence analysis of NANOG, OCT4, SOX2, and SSEA4 expression in transgene-residual (Kel6) and transgene-free (Kel6-R1) hiPSCs. **(B):** Quantitative RT-PCR analysis of ESC-specific genes (OCT3/4 and NANOG) in transgene-residual (Kel1 and Kel6) and transgene-free (Kel6-R1) hiPSCs. Each bar indicates the means and SEM. **(C):** Bisulfite sequencing of the OCT4 promoter region. Open and closed circles indicate unmethylated and methylated CpG dinucleotides, respectively. **(D):** Normal karyotype of the transgene-residual (Kel6) and transgene-free (Kel6-R1) hiPSCs. **(E):** We confirmed the differentiation capabilities of transgene-residual (Kel6) and transgene-free (Kel6-R1) hiPSCs into all three germ layers by direct differentiation in vitro: K14, ectoderm; AFP, endoderm; and desmin, mesoderm. Abbreviations: AFP, α-fetoprotein; hiPSCs-Retro, retrovirus-mediated reprogrammed human induced pluripotent stem cells (MRC-5); Tg+, transgene-residual; Tg−, transgene-free.

the epigenetic reprogramming status by the expression of stem cell markers, including *OCT4* and *NANOG*, and various differentiation markers in these iKCs by bisulfite sequencing analysis and real-time PCR, respectively. As expected, the DNA methylation status at *OCT4* promoter regions showed hypomethylation in the original hiPSCs (Kel6 and Kel6-R1) and hypermethylation in iKCs (iKC6 and iKC6-R1) (Fig. 3E). However, by comparing transgene-residual iKCs (iKC6) with transgene-free iKCs (iKC6-R1), the levels of DNA methylation were clearly higher in transgene-free iKCs (38% vs. 62%, respectively; Fig. 3E). To clarify the characteristics of iKCs, we performed single-cell gene expression profiling using Fluidigm dynamic arrays [21]. In line with the results of bisulfite sequencing analysis, stem cell markers, including *OCT4*, *SOX2*, *KLF4*, *MYC*, *LIN28*, and *NANOG*, were obviously expressed in transgene-residual iKCs (though at lower levels than those in hiPSCs), indicating that residual transgenes may have been reactivated in iKCs (Fig. 4; supplemental online Figs. 2, 4). Examination of the expression of keratinocyte-specific genes, including K5, K14, and dNp63, revealed higher expression in iKCs derived from transgene-free iPSCs than in those derived from transgene-residual iPSCs (both transposon- and retrovirus-based hiPSCs) (Fig. 4; supplemental online Fig. 5). On the other hand, K8 and K18, which are expressed during the early stage of epidermal cell lineages, were strongly positive in transgene-residual iKCs (Fig. 4). Based on these results, residual transgenes in hiPSCs could influence epidermal differentiation by reactivation, resulting in partial differentiation into K5/K14-positive keratinocytes.

For further examination, retrovirus-based hiPSCs (transgene residual) and hESCs (no transgenes) were differentiated into keratinocytes using the same protocols described in Figure 3A. At 4–5 weeks of differentiation, cells that could be maintained in keratinocyte-specific medium and that were positive for K5/K14 were obtained. Interestingly, iKCs derived from retrovirus-based hiPSCs morphologically resembled those derived from transgene-residual transposon-based hiPSCs, which showed a spindle-shaped morphology (Fig. 3B). The expression levels of stem cell marker genes, including *OCT4* and *NANOG*, in iKCs derived from retrovirus-based hiPSCs were as low as those in normal human somatic tissues (supplemental online Fig. 4). However, gene expression from the residual retrovirus vector was found to be reactivated in iKCs derived from retrovirus-based hiPSCs (supplemental online Fig. 6). Additionally, two other independent

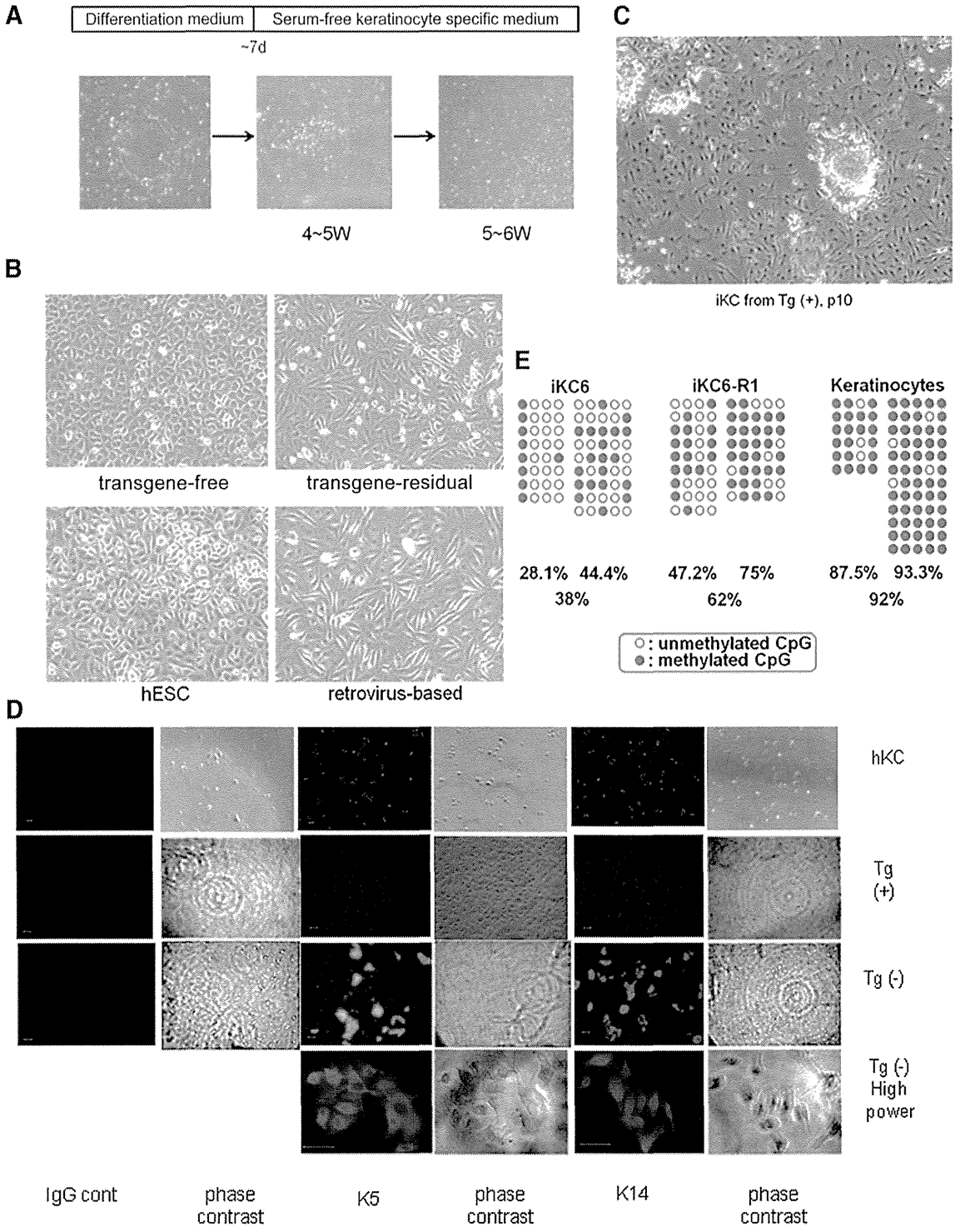

Figure 3. Keratinocytes induced from established hiPSCs. **(A):** Timeline of keratinocyte differentiation. Lower panels show representative photographs of cells at each stage (×40). **(B):** Morphology of cells derived from hiPSCs or hESCs indicated in panels, respectively (×100). **(C):** Morphology of cells derived from transgene-residual hiPSCs at a later passage (p10, ×40). **(D):** Immunofluorescence analysis of K5 and K14 expression in primary keratinocytes (hKCs) and iKCs derived from transgene-residual (Kel6) and transgene-free (Kel6-R1) hiPSCs. Scale bars = 50 μm. **(E):** Bisulfite sequencing of the OCT4 promoter region in iKCs and primary human keratinocytes. Open and closed circles indicate unmethylated and methylated CpG dinucleotides, respectively. Abbreviations: cont, control; d, days; hESC, human embryonic stem cell; hKC, human keratinocyte; IgG cont, IgG control; iKC, induced keratinocyte; Tg(+), transgene-residual; Tg(−), transgene-free; W, weeks.

hiPSC lines, Kel1 and Kel5 (Fig. 1D), both of which retain reprogramming transgenes, were subjected to the keratinocyte differentiation protocol. The Kel1- and Kel5-derived iKCs (iKC1 and iKC5, respectively) showed spindle-shaped morphologies similar to those of transgene-residual iKCs (iKC6) (Fig. 3B; data not shown).

Functional Properties of iKCs

As described above, the morphological and molecular phenotypes of iKCs derived from transgene-free hiPSCs or hESCs appeared to be more similar to those of normal human keratinocytes. Finally, we compared the tissue reconstitution potential of these iKCs using a three-dimensional (3D) culturing system for

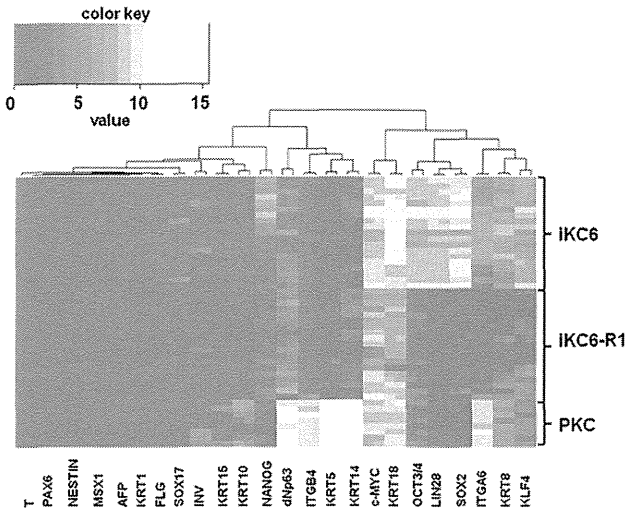

Figure 4. Single-cell gene expression analysis using the Fluidigm dynamic array. Single-cell gene expression profiling using Fluidigm dynamic arrays was performed. Heat maps depict the expression of genes differentially expressed between iKC6 (transgene residual) and iKC6-R1 (transgene-free) hiPSCs and primary human keratinocytes (control). Rows represent individual cells, and columns represent the evaluated genes. Genes highly expressed are shown in white, and genes with low expression are shown in red. Abbreviations: AFP, α-fetoprotein; dNp63, Δ N p63; iKC, induced keratinocyte; INV, involucrin; ITGA6, α6 integrin; ITGB4, β4 integrin; KRAT, keratin; PKC, primary human keratinocytes from neonatal male skin.

keratinocytes (CELLnTEC). According to the manufacturer's protocols, we performed the 3D culture experiments with both transgene-residual (iKC6) and -free (iKC6-R1) cell lines for approximately 21 days. As representatively shown in Figure 5A, iKC6-R1 cells successfully formed pluristratified epidermal structures in four of six experiments (67%), whereas no such structures were formed by iKC6 cells in any of the six experiments. In 3D culture, keratinocyte differentiation was evaluated by immunofluorescence staining of K14 and involucrin proteins (Fig. 5B). Lower layers of the pluristratified structure were positive for K14, whereas the upper layers were positive for involucrin, indicating in vitro reproduction of normal keratinocyte differentiation in vivo. A pluristratified structure was also formed by transgene-free hESCs in three of six experiments (50%) (Fig. 5C). In contrast, no such structures were formed by any of the transgene-residual hiPSC lines including iKC1 (seven experiments) and iKC-Retro (five experiments) (Fig. 5D). These results indicated that residual transgenes and their reactivation upon differentiation of keratinocytes from hiPSCs could critically influence not only the cellular phenotypes of such keratinocytes but also the functional properties of these cells for potential therapeutic use in regenerative medicine.

DISCUSSION

In this study, we present a direct comparison of the effects of excising reprogramming transgenes from hiPSCs in terms of cellular and molecular phenotypes and their potential for differentiation into keratinocytes in vitro. Comparison between hiPSCs generated by different induction methods, e.g., retrovirus-based (transgene-residual) hiPSCs versus Sendai virus-based (transgene-free) hiPSCs, did not reveal any effects of residual transgenes in hiPSCs. However, our *piggyBac* transposon-based method allowed generation of an isogenic pair of hiPSC lines with or without retention of the reprogramming transgenes, leading to a precise evaluation of the effects of residual transgenes in hiPSCs and their derivatives.

The present study showed that, in the presence of the residual transgenes that had been silenced in a pluripotent state before differentiation induction, the iPSCs underwent transcriptional reactivation of the exogenous genes and showed less efficient differentiation into keratinocytes. In fact, we compared the phenotypes and function of transgene-residual and -free hiPSCs and their derivatives (iKCs). In the undifferentiated state, there appeared to be no characteristic differences between transgene-residual and -free hiPSCs. Next, we differentiated these established hiPSCs into epidermal keratinocytes using a modified method published elsewhere [19, 20]. In morphological, gene expression, and functional analyses, we found that transgene-residual hiPSCs did not fully differentiate into keratinocytes. Single-cell analysis using the Fluidigm dynamic array revealed that the cells derived from transgene-residual hiPSCs remained in an early developmental stage of keratinocyte differentiation, i.e., the K8/K18-positive stage, which may be related to residual transgene reactivation and subsequent activation of endogenous pluripotency genes such as NANOG (Fig. 4). On the other hand, cells that resembled normal human keratinocytes were effectively induced from transgene-free hiPSCs (Figs. 3–5). Single-cell analysis showed that our keratinocyte differentiation method successfully induced epidermal lineage cells, because cell types belonging to other lineages were not detected as shown in Figure 4. However, the expression of keratinocyte-specific genes such as K5, K14, and dNP63 was still weak even in cells differentiated from transgene-free hiPSCs compared with that in primary human keratinocytes, indicating that better methods need to be established for keratinocyte differentiation. Another explanation is that a minor population (~10%) of iKC cells that expressed an extremely high level of K14 as shown in Figure 3D was included in the bulk analysis but excluded from the single-cell analysis by random selection (Fig. 4).

In terms of the relationship between residual transgenes and iPSC function, we found conflicting results in the present study. Previous reports have suggested that impaired silencing of transgenes in hiPSCs results in poor differentiation [22, 23]. Once the transgenes were silenced in iPSCs, these cells appeared to show a normal differentiation ability. Major et al. [24] reported that there are no differences between neuronal cell differentiation from transgene-residual or -free hiPSCs (induced by a lentiviral vector with Cre-loxp-mediated transgene excision system), and in that study, transgenes were silenced in hiPSCs. On the other hand, Toivonen et al. [25] reported that the reactivation of transgene in retrovirally generated hiPSCs affected the differentiation ability of these cells. The major problems of these previous contradicted reports were that hiPSCs generated from different methods (i.e., retrovirus-based and Sendai virus-based hiPSCs) had been compared. However, with our present situation, we could compare the phenotypes of transgene-residual and -free hiPSCs of the same genetic background, and this led to a precise evaluation of the effects of residual transgenes in hiPSCs and their derivatives. Thus, in our study, although the transgenes appeared to be silenced in hiPSCs, reactivation of the transgenes was obvious upon keratinocyte differentiation, leading to poor keratinocyte differentiation.

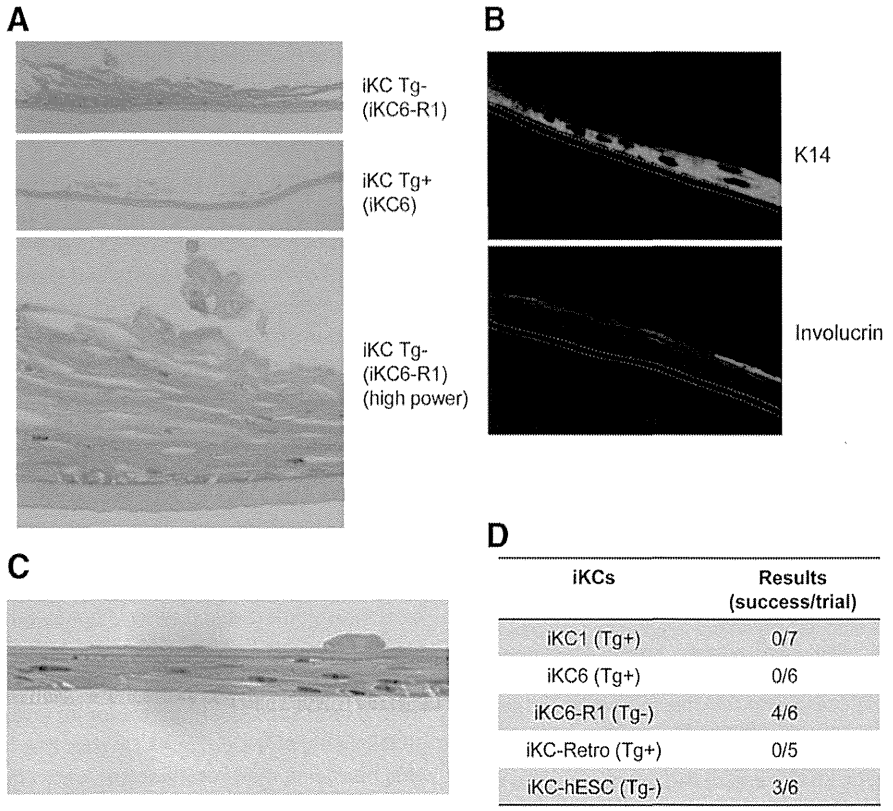

D

iKCs	Results (success/trial)
iKC1 (Tg+)	0/7
iKC6 (Tg+)	0/6
iKC6-R1 (Tg-)	4/6
iKC-Retro (Tg+)	0/5
iKC-hESC (Tg-)	3/6

Figure 5. Functional analysis of iKCs from hiPSCs. **(A):** Representative cross-sectional views of three-dimensional (3D) culture of iKCs using a 3D epidermal culture system (CELLnTEC). iKC6 and iKC6-R1 keratinocytes were generated from KeI6 (Tg+) and KeI6-R1 (Tg−) hiPSCs, respectively. Hematoxylin and eosin staining. Magnification is ×40 (top and middle) and ×200 (bottom). **(B):** Immunofluorescence analysis of K14 and involucrin expression in the reconstituted epidermis shown in **(A)** (×100). **(C):** Representative cross-sectional view of 3D culture of iKCs from hESCs. Hematoxylin and eosin staining is shown at ×100 magnification. **(D):** Results of 3D culture-based functionality tests of iKCs derived from various hiPSC lines or a hESC line. Abbreviations: hESC, human embryonic stem cell; iKC, induced keratinocyte; iKC-hESC, iKCs from hESCs; Tg+, transgene-residual; Tg−, transgene-free.

From another point of view, Itoh et al. [20] also reported that they selected cells in which the transgenes were not reactivated when evaluating their keratinocytes induced from retrovirus-based hiPSCs. Based on these results, including our own, the differentiation abilities of transgene-residual hiPSCs may be impaired, and this phenomenon may be more easily detected depending on the induced cell type. Specifically, residual transgenes tended to be reactivated more easily upon keratinocyte differentiation.

To further investigate whether reactivation of residual transgenes in hiPSCs was related to the method of derivation, namely transposon system specific, we differentiated retrovirus-based hiPSCs that were already confirmed to be pluripotent [26] (transgene residual) and hESCs (no transgenes) into epidermal keratinocytes using the same protocols and performed characteristic analyses of these cells. Morphologically, as expected, the cells differentiated from retrovirus-based hiPSCs showed a spindle shape resembling that of the differentiated transposon-based transgene-residual hiPSCs. On the other hand, cells differentiated from hESCs showed a cobblestone appearance that resembled the morphology of transposon-based transgene-free hiPSCs. Moreover, we clearly observed transgene reactivation in cells differentiated from retrovirus-based hiPSCs. These results strongly suggest that residual transgenes in hiPSCs can affect the differentiation ability, at least when differentiating into keratinocytes, through the reactivation of residual transgenes.

Moreover, the piggyBac transposon-based system for cellular reprogramming allowed efficient removal of reprogramming transgenes without residual exogenous sequences or any footprint mutations in the hiPSC genome. Even for establishment of human disease models in vitro, proper quality and safety precautions may be required because of the use of hiPSCs with viral transgene integration. Reactivation of any integrated transgene is one of the reasons for the oncogenicity of iPSCs [5–8]. Furthermore, transgene integration itself causes insertional mutagenesis [9]. Therefore, several methods have been developed to generate iPSCs, other than retrovirus-based methods, including those using plasmids [27], recombinant proteins [28], episomal viral vectors [29], and mRNA [30, 31] for derivation of transgene integration-free iPSCs. Among these methods, although the Sendai viral vector is now widely used to generate transgene integration-free iPSCs, it can be quite difficult to show that there is no residual virus in the cells. Therefore, among the various methods, we selected the *piggyBac* transposon system to generate hiPSCs.

Conclusion

Our results have significant implications for the clinical use (or even laboratory use) of hiPSCs. Specifically, we confirmed that transgene-residual hiPSCs are not suitable for clinical use and that transgene integration-free hiPSCs are necessary. The timing of integrated transgene reactivation cannot be predicted, and thus, transgene-free hiPSCs are more appropriate not only for

clinical use and also laboratory use; otherwise the results may be affected. In addition, our *piggyBac* transposon system for the creation of hiPSCs may be a powerful approach, especially for clinical use.

Acknowledgments

We thank K. Nishida for the histological analysis and M. Tokunaga for single-cell sorting. This work was supported in part by Grants-in-Aid for Scientific Research from the Ministry of Education, Culture, Sports, Science and Technology of Japan. This work was also supported in part by a grant from the Takeda Science Foundation. Human embryonic stem cells were used following the guidelines for use of human embryonic stem cells of the Ministry of Education, Culture, Sports, Science and Technology of Japan.

Author Contributions

K.I. and J.T.: conception and design, collection and/or assembly of data, data analysis and interpretation, manuscript writing; C.K. and K.H.: collection and/or assembly of data, data analysis and interpretation, manuscript writing; K. Yusa: construction of reprogramming vectors, manuscript writing; Y.Y., K. Yamauchi, and H.S.: collection and/or assembly of data; H.Y. and I.K.: conception and design; M.T., N.K., H.O., Y.M., H.A., and A.U.: provision of retroviral-based hiPSCs.

Disclosure of Potential Conflicts of Interest

The authors indicate no potential conflicts of interest.

References

1 Yamanaka S. Strategies and new developments in the generation of patient-specific pluripotent stem cells. Cell Stem Cell 2007;1:39–49.
2 Takahashi K, Yamanaka S. Induction of pluripotent stem cells from mouse embryonic and adult fibroblast cultures by defined factors. Cell 2006;126:663–676.
3 Takahashi K, Tanabe K, Ohnuki M et al. Induction of pluripotent stem cells from adult human fibroblasts by defined factors. Cell 2007; 131:861–872.
4 Jones JM, Thomson JA. Human embryonic stem cell technology. Semin Reprod Med 2000; 18:219–223.
5 Okita K, Ichisaka T, Yamanaka S. Generation of germline-competent induced pluripotent stem cells. Nature 2007;448:313–317.
6 Nakagawa M, Koyanagi M, Tanabe K et al. Generation of induced pluripotent stem cells without Myc from mouse and human fibroblasts. Nat Biotechnol 2008;26:101–106.
7 Hochedlinger K, Yamada Y, Beard C et al. Ectopic expression of Oct-4 blocks progenitor-cell differentiation and causes dysplasia in epithelial tissues. Cell 2005;121:465–477.
8 Foster KW, Liu Z, Nail CD et al. Induction of KLF4 in basal keratinocytes blocks the proliferation-differentiation switch and initiates squamous epithelial dysplasia. Oncogene 2005;24:1491–1500.
9 Nair V. Retrovirus-induced oncogenesis and safety of retroviral vectors. Curr Opin Mol Ther 2008;10:431–438.
10 Cary LC, Goebel M, Corsaro BG et al. Transposon mutagenesis of baculoviruses: Analysis of Trichoplusia ni transposon IFP2 insertions within the FP-locus of nuclear polyhedrosis viruses. Virology 1989;172:156–169.
11 Ding S, Wu X, Li G et al. Efficient transposition of the piggyBac (PB) transposon in mammalian cells and mice. Cell 2005;122:473–483.
12 Fraser MJ, Ciszczon T, Elick T et al. Precise excision of TTAA-specific lepidopteran transposons piggyBac (IFP2) and tagalong (TFP3) from the baculovirus genome in cell lines from two species of Lepidoptera. Insect Mol Biol 1996; 5:141–151.
13 Yusa K, Rad R, Takeda J et al. Generation of transgene-free induced pluripotent mouse stem cells by the piggyBac transposon. Nat Methods 2009;6:363–369.
14 Kaji K, Norrby K, Paca A et al. Virus-free induction of pluripotency and subsequent excision of reprogramming factors. Nature 2009; 458:771–775.
15 Woltjen K, Michael IP, Mohseni P et al. piggyBac transposition reprograms fibroblasts to induced pluripotent stem cells. Nature 2009;458:766–770.
16 van der Weyden L, Adams DJ, Harris LW et al. Null and conditional semaphorin 3B alleles using a flexible puroDeltatk loxP/FRT vector. Genesis 2005;41:171–178.
17 Suemori H, Yasuchika K, Hasegawa K et al. Efficient establishment of human embryonic stem cell lines and long-term maintenance with stable karyotype by enzymatic bulk passage. Biochem Biophys Res Commun 2006;345: 926–932.
18 Szymczak AL, Workman CJ, Wang Y et al. Correction of multi-gene deficiency in vivo using a single "self-cleaving" 2A peptide-based retroviral vector. Nat Biotechnol 2004;22:589–594.
19 Guenou H, Nissan X, Larcher F et al. Human embryonic stem-cell derivatives for full reconstruction of the pluristratified epidermis: A preclinical study. Lancet 2009;374:1745–1753.
20 Itoh M, Kiuru M, Cairo MS et al. Generation of keratinocytes from normal and recessive dystrophic epidermolysis bullosa-induced pluripotent stem cells. Proc Natl Acad Sci USA 2011;108:8797–8802.
21 Citri A, Pang ZP, Südhof TC et al. Comprehensive qPCR profiling of gene expression in single neuronal cells. Nat Protoc 2011;7: 118–127.
22 Sommer CA, Sommer AG, Longmire TA et al. Excision of reprogramming transgenes improves the differentiation potential of iPS cells generated with a single excisable vector. Stem Cells 2010;28:64–74.
23 Ramos-Mejía V, Montes R, Bueno C et al. Residual expression of the reprogramming factors prevents differentiation of iPSC generated from human fibroblasts and cord blood CD34+ progenitors. PLoS ONE 2012;7: e35824.
24 Major T, Menon J, Auyeung G et al. Transgene excision has no impact on in vivo integration of human iPS derived neural precursors. PLoS ONE 2011;6:e24687.
25 Toivonen S, Ojala M, Hyysalo A et al. Comparative analysis of targeted differentiation of human induced pluripotent stem cells (hiPSCs) and human embryonic stem cells reveals variability associated with incomplete transgene silencing in retrovirally derived hiPSC lines. Stem Cells Translational Medicine 2013;2: 83–93.
26 Makino H, Toyoda M, Matsumoto K et al. Mesenchymal to embryonic incomplete transition of human cells by chimeric OCT4/3 (POU5F1) with physiological co-activator EWS. Exp Cell Res 2009;315:2727–2740.
27 Okita K, Nakagawa M, Hyenjong H et al. Generation of mouse induced pluripotent stem cells without viral vectors. Science 2008;322: 949–953.
28 Zhou H, Wu S, Joo JY et al. Generation of induced pluripotent stem cells using recombinant proteins. Cell Stem Cell 2009; 4:381–384.
29 Fusaki N, Ban H, Nishiyama A et al. Efficient induction of transgene-free human pluripotent stem cells using a vector based on Sendai virus, an RNA virus that does not integrate into the host genome. Proc Jpn Acad Ser B Phys Biol Sci 2009;85:348–362.
30 Miyoshi N, Ishii H, Nagano H et al. Reprogramming of mouse and human cells to pluripotency using mature microRNAs. Cell Stem Cell 2011;8:633–638.
31 Subramanyam D, Lamouille S, Judson RL et al. Multiple targets of miR-302 and miR-372 promote reprogramming of human fibroblasts to induced pluripotent stem cells. Nat Biotechnol 2011;29:443–448.

See www.StemCellsTM.com for supporting information available online.

Published in final edited form as:
Nat Chem Biol. 2014 August ; 10(8): 632–639. doi:10.1038/nchembio.1552.

Notch inhibition allows oncogene independent generation of iPS cells

Justin K. Ichida[#1,2,9], **Julia TCW**[#1,2,3], **Luis A. Williams**[1,2], **Ava C. Carter**[1,2], **Yingxiao Shi**[9], **Marcelo T. Moura**[1,2], **Michael Ziller**[1,4], **Sean Singh**[1,2], **Giovanni Amabile**[5], **Christoph Bock**[1,4], **Akihiro Umezawa**[6], **Lee L. Rubin**[1], **James E. Bradner**[7,8], **Hidenori Akutsu**[6], **Alexander Meissner**[1,4], and **Kevin Eggan**[1,2,3]

[1] Harvard Stem Cell Institute, Department of Stem Cell and Regenerative Biology, Harvard University, Cambridge, MA 02138, USA

[2] Howard Hughes Medical Institute and Stanley Center for Psychiatric Research

[3] Department of Molecular and Cellular Biology, Harvard University, Cambridge, MA 02138, USA

[4] Broad Institute of MIT and Harvard, 7 Cambridge Center, Cambridge, Massachusetts 02142, USA

[5] Harvard Stem Cell Institute, Harvard Medical School, Boston, MA

[6] Department of Reproductive Biology, National Research Institute for Child Health and Development, 2-10-1 Okura, Setagaya, Tokyo 157-8535, USA

[7] Department of Medical Oncology, Dana-Farber Cancer Institute, 450 Brookline Avenue, Boston, MA 02215, USA

[8] Department of Medicine, Harvard Medical School, 25 Shattuck Street, Boston, MA 02115, USA

[9] Department of Stem Cell Biology and Regenerative Medicine, University of Southern California, 1425 San Pablo Street, Los Angeles, CA 90033, USA

[#] These authors contributed equally to this work.

Abstract

The reprogramming of somatic cells to pluripotency using defined transcription factors holds great promise for biomedicine. However, human reprogramming remains inefficient and relies either on the use of the potentially dangerous oncogenes KLF4 and CMYC or the genetic inhibition of the

Correspondence and requests for materials should be addressed to K.E. (keggan@scrb.harvard.edu), A.M. (alexander_meissner@harvard.edu), or H.A. (akutsu-h@ncchd.go.go.jp)..

Author Contributions

A.M. and J.E.B. hypothesized Notch inhibition might aid reprogramming. J.K.I., J.T., A.M., A.U., L.L.R., and K.E. designed reprogramming and mechanistic experiments to test the hypothesis. J.K.I., J.T., A.C.C., L.A.W., Y.S., M.T.M., S.S., G.A., and H.A. performed reprogramming experiments and characterization of the iPSCs. C.B. and M.Z. performed bioinformatic analysis of transcriptional data characterizing the iPSCs. J.K.I., J. T., A.C.C., and Y.S. performed experiments to determine the mechanism of action of DAPT and Notch inhibition in reprogramming. K.E., J.K.I. and J.T. discovered and confirmed the mechanism of action of DAPT. K.E. and J.K.I. wrote the paper. All helped in paper revision.

The authors declare no competing financial interests.

Accession numbers

Microarray data have been submitted to the GEO repository with accession number GSE35090.

tumor suppressor gene p53. We hypothesized that inhibition of signal transduction pathways that promote differentiation of the target somatic cells during development might relieve the requirement for non-core pluripotency factors during iPSC reprogramming. Here, we show that inhibition of Notch significantly improves the efficiency of iPSC generation from mouse and human keratinocytes by suppressing p21 in a p53-independent manner and thereby enriching for undifferentiated cells capable of long-term self-renewal. Pharmacological inhibition of Notch enabled routine production of human iPSCs without KLF4 and CMYC while leaving p53 activity intact. Thus, restricting the development of somatic cells by altering intercellular communication enables the production of safer human iPSCs.

Use of the potent oncogenes *KLF4* and *CMYC* in the generation of induced pluripotent stem cells (iPSCs) limits their translational utility [1,2]. Currently, elimination of these genes during human iPSC reprogramming requires suppression of p53 activity [2-16], which in turn results in the accumulation of genetic mutations in the resulting iPSCs [8]. Therefore, there remains a real need for reprogramming approaches that enable iPSC generation without the use of *KLF4* and *CMYC* while leaving p53 activity intact.

In part to address this need, several groups have undertaken chemical screens to identify small molecules that can improve reprogramming [17-21]. Thus far, the majority of active compounds are thought to improve reprogramming by inhibiting chromatin-modifying enzymes or by reinforcing the transcriptional network associated with the pluripotent state [17-22]. Consistent with their proposed mechanisms of action, these chemicals generally function in cellular intermediates that arise late in reprogramming, catalyzing their final conversion into iPSCs [19,22]. It is currently unclear whether known chemicals are sufficient for generating iPSCs from adult human cells, which are consistently more difficult to reprogram than mouse embryonic fibroblasts [23].

Given the likely need for additional reprogramming chemicals and the knowledge that most known compounds act late in this process, we reasoned it would be valuable to identify small molecules that improve reprogramming by acting early, perhaps within the somatic cells themselves. We reasoned that one approach towards this goal would be to identify chemicals that could modulate signal transduction cascades in somatic cell populations to enrich for those cells with an enhanced capacity for reprogramming. We reasoned that if such compounds could be identified, they might expand the translational utility of chemical reprogramming.

It has been recognized that the extent of a target cell's differentiation is an important determinant of the efficiency by which it can be reprogrammed [24-26]. We therefore hypothesized that chemically driving somatic cells into a more potent "stem cell" state might improve their reprogramming. To test this hypothesis, we chose to ask whether known chemical inhibitors of the Notch signaling pathway could aid in reprogramming.

The Notch signaling pathway is highly conserved and regulates the proliferation and differentiation of many distinct progenitor cell and stem cell types [27]. Notch ligands are generally transmembrane proteins that require contact between two cells in order to mediate signal transduction [28]. In skin, Notch promotes differentiation by directly activating *p21*

expression, which in turn blocks proliferation and induces the differentiation of keratinocyte stem cell populations [29,30]. We therefore hypothesized that inhibition of Notch in keratinocytes might enhance iPSC generation by inhibiting differentiation and enriching more easily reprogrammed progenitor cells. We also felt that keratinocytes were an attractive model for testing our hypothesis because if Notch inhibition did have an effect, it could be immediately translated to the production of patient-specific iPSCs [31,32].

Here, we show that Notch inhibition significantly improves the efficiency of iPSC generation from mouse and human keratinocytes by suppressing p21 and thereby enriching undifferentiated cells with increased reprogramming potential. In addition, pharmacological inhibition of Notch enabled the efficient production of human iPSCs without *KLF4* and *CMYC* while leaving p53 activity intact, resulting in the production of safer human iPSCs.

Results

DAPT treatment promotes keratinocyte reprogramming

Notch signaling is activated by the γ-secretase complex, which cleaves the membrane-tethered Notch receptor upon ligand binding and generates a free intracellular domain that can translocate to the nucleus and modulate transcription [27]. It has previously been shown that the γ-secretase inhibitor DAPT (Fig. 1a) can block Notch signaling in mouse keratinocytes [33]. As expected, 10 μM DAPT treatment of both neonatal mouse and human keratinocytes transduced with the iPSC reprogramming factors increased abundance of the full-length Notch receptor, reduced levels of cleaved Notch intracellular domain (NICD) (Supplementary Results, Supplementary Fig. 1a), and decreased expression of the Notch-target genes *Hey1, Hes1, Hes5*, and *Col6a1* (Supplementary Fig. 1b).

To determine whether inhibition of Notch could increase the efficiency of reprogramming, we transduced *Oct4*::GFP mouse or human keratinocytes with *Oct4, Sox2, Klf4*, and *cMyc* and cultured the resulting cells for 25 days either in the presence or absence of DAPT. We found that the addition of 10 μM DAPT led to a significant, 4-fold increase in the number of resulting *Oct4::*GFP+ mouse and NANOG+/TRA-1-81+ human iPSC colonies (Fig. 1b).

We wondered whether this increase in reprogramming activity might allow the generation of iPSCs from keratinocytes without *Klf4* and *cMyc*. Indeed, although transduction of *Oct4* and *Sox2* alone were not sufficient to induce keratinocyte reprogramming, *Oct4* and *Sox2* combined with DAPT treatment routinely yielded mouse and human iPSC colonies (Figs. 1c,d and Supplementary Fig. 2a). This effect was specific to *Oct4* and *Sox2*-transduced cells because other 2-factor combinations did not yield iPSCs in the presence of DAPT (Fig. 1c).

To determine whether these putative iPS cell lines were pluripotent, we subjected them to a "scorecard" assay for pluripotency that we recently developed [34]. We found that these cell lines were indeed composed of pluripotent cells and that they performed comparably to human embryonic stem cells (ESCs) in their expression of pluripotency-associated genes and differentiation propensities (Supplementary Figs 2b, c). To further confirm their differentiation capacity, we also injected the *OCT4, SOX2* + DAPT human cells into immunocompromised mice and found that they readily formed teratomas containing

differentiated cells (Fig. 1e). Moreover, when injected into blastocysts, the *Oct4, Sox2* + DAPT mouse cells contributed to the development of chimeric mice (Supplementary Fig. 2d), including the germ-line (Supplementary Fig. 2e).

Many applications of iPS cells would require the DAPT-dependent generation of *KLF4* and *CMYC*-free iPSCs from adult keratinocytes. Therefore, we determined if DAPT treatment increased the reprogramming potential of adult human keratinocytes. As with mouse and human neonatal keratinocytes, we found that DAPT treatment of *KLF4, SOX2, OCT4*, and *CMYC*-transduced adult human keratinocytes significantly improved their rate of reprogramming (Supplementary Fig. 2f) and also enabled the generation of iPSCs with just *OCT4* and *SOX2* (Fig. 1f, Supplementary Fig. 2g). The scorecard assay again verified that these 2-factor iPSCs were pluripotent (Supplementary Figs 2b, c). Together, these results demonstrate that DAPT reliably enables the generation of *bona fide* mouse and human iPSCs from keratinocytes without *KLF4* and *CMYC*.

Notch inhibition promotes reprogramming

Our results thus far suggest that antagonizing Notch signaling in keratinocytes may promote their conversion into iPSCs. To begin verifying that NOTCH was indeed the functional target of DAPT during reprogramming, we tested a structurally distinct γ-secretase inhibitor, DBZ [35](Fig. 2a), for activity in iPSC generation. When we treated human keratinocytes with DBZ, we observed significant reductions in the levels of the intracellular domain of the NOTCH receptor (Supplementary Fig.1a) and the NOTCH-dependent genes *HES1* and *HES5* (Supplementary Fig. 3a), indicating that DBZ administration inhibited NOTCH signaling. Consistent with the notion that NOTCH inhibition increases the rate of reprogramming, DBZ significantly stimulated the formation of human iPSC colonies (Fig. 2b).

Both DBZ and DAPT could have effects on the processing of unidentified γ-secretase substrates that are distinct from NOTCH, which might also impact reprogramming efficiency. If the beneficial effects of DAPT on reprogramming were being mediated through the specific inhibition of NOTCH signaling rather than through some other target of γ-secretase, then we reasoned that constitutive activation of NOTCH signaling should eliminate the beneficial effect of DAPT. Consistent with this notion, we found that overexpression of the NOTCH intracellular domain (Supplementary Fig. 3b) stimulated the expression of NOTCH-target genes (Supplementary Fig. 3c) and completely blocked the positive effects of DAPT on reprogramming (Fig. 2c). Conversely, we reasoned that antagonizing the transcriptional activity of NOTCH should increase the rate of keratinocyte reprogramming. Indeed, when we suppressed NOTCH activity by overexpressing a dominant-negative form of *MAML1* (Fig. 2d), a transcriptional co-activator for NOTCH [36,37], we observed an increase in iPSC generation from keratinocytes transduced with all 4 reprogramming factors (Fig. 2e). Therefore, we conclude that the inhibition of NOTCH signaling promotes the reprogramming of both human and mouse keratinocytes.

In order to understand how Notch inhibition promotes iPSC generation, we first determined when in the reprogramming process it was required. We treated mouse keratinocytes with DAPT either before or both before and after transduction with reprogramming factors.

While treatment both before and after transduction yielded a 4-fold increase in iPSC generation, we found that pre-treatment alone resulted in a significant 2.5-fold enhancement in reprogramming efficiency (Supplementary Fig. 4a). To more precisely pinpoint the effective post-transduction treatment window, we transduced human keratinocytes with *KLF4, OCT4, SOX2*, and *CMYC* and administered DAPT or DBZ from days 1-6, 6-11, 11-16, or 1-16 after viral infection (Figs 3a-c). Chemical inhibition of NOTCH signaling was most effective during early time points, significantly increasing iPSC generation when used from days 1-6 and 6-11 (Figs 3b, c). In contrast, a later treatment from days 11-16 had little effect on reprogramming (Figs 3b, c). Together, these results indicate that Notch inhibition can act on the starting keratinocytes and at early time points just after the initiation of transcription factor overexpression to enhance reprogramming.

Notch inhibition acts by suppressing p21 expression

One way that Notch inhibition could promote iPSC formation is by activating the expression of the reprogramming transcription factors from their endogenous loci. However, when we treated human keratinocytes with DAPT and analyzed their gene expression, we found that levels of *KLF4, OCT4*, and *CMYC* actually decreased and *SOX2* did not significantly change (Supplementary Fig. 4b).

In the mammalian epidermis, Notch signaling functions as a switch that directly activates *p21* transcription, which in turn forces keratinocytes to exit the cell cycle and begin differentiating [38]. To determine if chemical inhibition of Notch signaling in keratinocytes might be enhancing their reprogramming potential by suppressing *p21*, we measured p21 levels in human keratinocytes in the presence and absence of DAPT. Consistent with previous reports [38], we found that Notch inhibition decreased the levels of *p21* mRNA and protein in these cells (Supplementary Fig. 4c, Fig. 3d). In addition, DAPT treatment slightly decreased the level of FLAG-tagged p21 protein expressed by an exogenous retrovirus, indicating that Notch may also regulate p21 post-transcriptionally (Supplementary Figs. 4d, e). Consistent with these observations, Notch inhibition suppressed expression of *INVOLUCRIN*, which is expressed in more differentiated keratinocytes (Fig. 3e).

To verify that Notch inhibition promotes iPSC reprogramming by suppressing p21, we performed 2-factor (*Oct4* and *Sox2*) and 4-factor reprogramming in keratinocytes with p21 siRNA/shRNA in the presence or absence of DAPT. Mouse keratinocytes transduced with *Klf4, Sox2, Oct4*, and *cMyc* showed a similar increase in iPSC generation when treated with either 2.5 μm DAPT or p21 siRNA (Supplementary Fig. 4f). The efficiency of reprogramming with these two methods was not significantly different (Supplementary Fig. 4f), and treating with DAPT in the presence of the p21 siRNA did not produce a significant increase in iPSC formation (Supplementary Fig. 4f). Similarly, suppression of p21 by shRNA (Supplementary Figs 4g, h) enabled the generation of iPSCs from human keratinocytes transduced with 2 or 4 factors at rates equivalent to DAPT treatment (Figs 3f, g). Again, supplementing p21 knockdown with DAPT treatment did not result in a significant increase in iPSC formation (Figs 3f, g). These results indicate that p21 suppression and DAPT have similar effects on iPSC generation from keratinocytes and that DAPT does not provide an additional advantage over p21 suppression alone.

If Notch inhibition and p21 suppression indeed blocks keratinocyte differentiation, the p21-treated keratinocytes would be predicted to display an increase in their long-term proliferative capacity [39]. The ability to form large colonies on collagen demonstrates the ability of keratinocytes to self-renew extensively and is a functional property unique to undifferentiated cells of this lineage [39]. In contrast, differentiated keratinocytes senesce after only a few rounds of division and do not form colonies [39]. DAPT treatment of human keratinocytes for 6 days significantly increased the number of cells capable of forming large colonies when cultured for an additional 14 days in the absence of the chemical (Supplementary Fig. 4i). The resulting 4-fold increase in colony formation rate was similar in magnitude to the elevation in iPSC generation with DAPT treatment (Fig. 1b). To determine if this increased self-renewal capacity was indeed promoting reprogramming, we transduced keratinocytes with p21 to limit their replication and attempted to reprogram them either with or without DAPT. The forced p21 expression severely impaired the self-renewal potential of the keratinocytes (Supplementary Fig. 4j) and inhibited iPSC formation after transduction with the 4 reprogramming factors and treatment with DAPT (Fig. 3h).

Because Notch inhibition does not promote fibroblast replication [40], if this is the mechanism by which DAPT improves reprogramming, we would not expect chemical treatment to affect mouse embryonic fibroblast [41] reprogramming [41]. Indeed, DAPT treatment of MEFs transduced with all 4 reprogramming factors did not affect the rate of iPSC generation (Supplementary Fig. 4k). Together, these results demonstrate that Notch inhibition promotes iPSC generation from keratinocytes by repressing their differentiation and enhancing their long-term replicative potential through p21 suppression.

Efficient reprogramming with Notch and DOT1L inhibition

Knowing that Notch inhibition enhances iPSC generation through this unique mechanism, we next wanted to compare its activity to previously described reprogramming molecules that act through other mechanisms [17,42-44] and identify any that DAPT might synergize with. When we transduced human neonatal keratinocytes with *KLF4, SOX2, OCT4*, and *CMYC* and treated them with various combinations of compounds shown to enhance reprogramming in other reports, including an activator of 3'-phosphoinositide-dependent kinase-1 (PDK1)[17], inhibitors of TGF-β, MEK, and GSK3β signaling [17], histone deacetylase inhibitors [17,42], histone methyltransferase inhibitors [17,44], and a DNA methyltransferase inhibitor [43], we found that DAPT treatment was the most potent at enhancing reprogramming (Fig. 4a). This remained true when we attempted reprogramming with only *OCT4* and *SOX2* (Fig. 4b).

However, an inhibitor of the histone methyltransferase DOT1L (iDOT1L) synergized *OCT4, SOX2* and DAPT to elevate the rate of iPSC generation by 10-fold over the rate with *OCT4, SOX2* and DAPT alone, making it even more efficient than 4-factor reprogramming either with or without DAPT (Fig. 4b). The *OCT4* + *SOX2* + DAPT + iDOT1L colonies could be readily expanded and maintained NANOG and TRA-1-81 expression (Fig. 4c). These data indicate that Notch inhibition is a potent enhancer of reprogramming in keratinocytes that can synergize with chromatin-modifying compounds to induce pluripotency at a high efficiency with only *OCT4* and *SOX2*.

Notch inhibition does not compromise p53 activity

Previous studies of p53 and p21 in reprogramming have suggested that ectopic overexpression of reprogramming transcription factors can activate p53, which then induces either apoptosis or the expression of p21, thus inhibiting reprogramming [3,6]. Because suppression of the p53 pathway greatly facilitates iPSC generation, this approach has become an important part of reprogramming methods that reduce or eliminate integrating exogenous transcription factors [3,4]. However, because p53 inhibition allows the accumulation of genetic mutations during reprogramming [8], alternative approaches for increasing reprogramming efficiencies would be desirable. We therefore next asked whether Notch inhibition promotes reprogramming through a p53-dependent or independent pathway by analyzing the effects of DAPT and DBZ treatment on p53 and its target genes. First, we confirmed the finding that transduction with the iPSC reprogramming factors stimulated p53 activity (Fig. 5a). Chemical inhibition of Notch signaling in both human and mouse keratinocytes did not reduce the expression of p53 at the protein or mRNA level either before or after transduction with the reprogramming factors (Figs 5b,c and Supplementary Figs 5a, b). Moreover, transcriptional analysis of DAPT-treated human and mouse keratinocytes revealed that the mRNA levels of the p53 target genes *Dr5, Puma*, and *Fas* were not decreased (Fig. 5c and Supplementary Figs 5a, b), supporting the notion that p53 activity was not suppressed by Notch inhibition.

To further confirm that DAPT treatment did not suppress p53 activity, we performed reprogramming experiments with and without DAPT after UV irradiation. UV exposure causes DNA damage, which in turn reduces reprogramming efficiencies by inducing p53-dependent apoptosis [8]. However, p53-deficient cells are resistant to the negative effects of UV irradiation on reprogramming [8]. Therefore, if p53 activity was maintained in DAPT-treated cultures, then we would expect a sharp decrease in reprogramming efficiency after UV irradiation. As a control for p53-deficiency, we performed 4-factor reprogramming with or without UV irradiation using keratinocytes in which we overexpressed a dominant-negative form of p53 (p53DD) [3] that suppressed p53 activity as evidenced by a decrease in the expression levels of p53-dependent target genes (Supplementary Fig. 5c). As expected, UV exposure did not impact the rate of iPSC generation when p53DD was expressed, functionally demonstrating that p53 activity was indeed impaired (Fig. 5d). In contrast, in the absence of p53DD overexpression, UV exposure sharply reduced the number of iPSCs generated in DMSO-treated cultures (Fig. 5d). Similarly, UV irradiation severely diminished the number of iPSC colonies in DAPT-treated cultures again suggesting that Notch inhibition does not suppress p53 activity during reprogramming (Fig. 5d).

Although the difference in reprogramming efficiency in p53-deficient versus DAPT-treated keratinocytes was clearly evident when UV irradiation was used to induce DNA damage, we next determined whether DNA damage was measurably influenced by DAPT treatment under normal reprogramming conditions. To test this, we quantified phosphorylated histone H2AX (γH2AX) expression in 4-factor-transduced human keratinocytes treated with DAPT, p53DD, or p53 shRNA. Histone H2AX becomes phosphorylated in response to double strand DNA breaks, making it a reliable marker of DNA damage [8]. Pan-nuclear γH2AX expression results from replication-induced damage and could indicate insults sustained

during reprogramming [8]. We found that 10 days after transduction, pan-nuclear γH2AX staining was significantly elevated in cultures treated with p53DD or p53 shRNA, which is consistent with a previous study in which elevated rates of DNA damage were observed in p53-deficient cells during reprogramming and in the resulting iPSCs [8] (Fig. 5e and Supplementary Figs 5d-f). The DAPT-treated cells, however, maintained low cell numbers with pan-nuclear γH2AX expression that were similar to the control cultures (Fig. 5e and Supplementary Fig. 5f). These results suggest that, in contrast to p53-deficiency, DAPT treatment did not promote the survival and reprogramming of cells with DNA damage.

To confirm that Notch inhibition does not prevent the apoptosis of compromised cells during reprogramming, we measured the fraction of TUNEL-positive nuclei in DAPT-treated cultures. Despite high rates of DNA damage in the p53-deficient reprogramming cultures, the percentage of TUNEL-positive nuclei was greatly reduced compared to a wild-type control, indicating that inactivation of p53 permitted the survival of cells with compromised genomes (Fig. 5f). In contrast, the percentage of TUNEL-positive cells was not significantly reduced by DAPT treatment (Fig. 5f).

In order to determine if DAPT enabled the efficient generation of iPSCs that displayed improved genomic integrity relative to their counterparts made through p53 suppression, we measured the copy number variation in iPSC lines made with DAPT or p53DD. Consistent with the γH2AX and TUNEL staining results, we found that iPSC lines derived in the presence of p53DD possessed an average of 4 indels/line, while iPSCs derived with a control GFP vector or 10 μm DAPT contained only 1 or .5 indels/line, respectively (Fig. 5g and Supplementary Fig. 6). Together, these experiments show that DNA damage is present during normal reprogramming conditions and that inhibition of p53 allows cells with damaged genomic material to persist. In contrast, Notch inhibition enhances reprogramming without compromising genomic integrity or promoting the survival of iPSCs that have undergone DNA damage.

Discussion

In summary, our findings suggest that signaling through the Notch pathway is a significant impediment to the early stages of the reprogramming of both mouse and human keratinocytes into iPSCs (Figure 6). Importantly, the mechanism by which Notch signaling likely inhibits reprogramming of mouse and human cells is by activating p21 independently of p53. Consistent with this hypothesis, treatment of reprogramming cultures with the γ-secretase inhibitors DAPT and DBZ reduced the levels of intracellular Notch and increased colony forming potential, leading to an increase in the rate of iPSC formation. Suppression of p21 expression by siRNA/shRNA was sufficient to replace Notch inhibition in reprogramming, and exogenous p21 blocked the beneficial effects of DAPT. Importantly, the resulting improvement in reprogramming activity did not come at the expense of a reduction in p53 activity or increased genomic instability (Figure 6).

Our findings have immediate and practical ramifications for the improved production of patient-specific human iPSCs. When taken together, our studies show that through pharmacological inhibition of NOTCH, it is routinely possible to produce human iPSCs with